

Mean-field study of the heavy-fermion metamagnetic transition

S. Viola Kusminskiy,¹ K. S. D. Beach,^{2,3} A. H. Castro Neto,¹ and D. K. Campbell¹

¹*Department of Physics, Boston University, 590 Commonwealth Avenue, Boston, Massachusetts 02215, USA*

²*Institut für Theoretische Physik und Astrophysik, Universität Würzburg, Am Hubland, D-97074 Würzburg, Germany*

³*Department of Physics, University of Alberta, Edmonton, Alberta, Canada T6G 2D7*

(Received 16 November 2007; published 18 March 2008)

We investigate the evolution of the heavy-fermion ground state under application of a strong external magnetic field. We present a richer version of the usual hybridization mean-field theory that allows for hybridization in both the singlet and triplet channels and incorporates a self-consistent Weiss field. We show that for a magnetic field strength B^* , a filling-dependent fraction of the zero-field hybridization gap, the spin up quasiparticle band becomes fully polarized—an event marked by a sudden jump in the magnetic susceptibility. The system exhibits a kind of quantum rigidity in which the susceptibility (and several other physical observables) is insensitive to further increases in field strength. This behavior ends abruptly with the collapse of the hybridization order parameter in a first-order transition to the normal metallic state. We argue that the feature at B^* corresponds to the “metamagnetic transition” in YbRh_2Si_2 . Our results are in good agreement with recent experimental measurements.

DOI: 10.1103/PhysRevB.77.094419

PACS number(s): 75.20.Hr, 75.30.Kz, 71.27.+a, 71.10.Fd

I. INTRODUCTION

The Kondo lattice model away from half filling describes what is called a *heavy metal*—a Fermi liquid state distinguished by its high magnetic susceptibility and large Sommerfeld coefficient. The properties of this state are a consequence of the hybridization between the localized impurity spins (f electrons) and the conduction electrons (c electrons). The f electrons are said to delocalize in the sense that the Luttinger volume is now comprised of the sum of both species, c and f .¹ The shallow dispersion of the resulting quasiparticles leads to a renormalization of the effective mass to very large values.² Materials that belong to this category are usually rare-earth intermetallic compounds, in which $4f$ or $5f$ electrons act as magnetic impurities embedded in a metallic host.³

It is known that a sufficiently strong magnetic field will destroy the heavy-fermion state. Measurements in applied field often reveal a so-called metamagnetic transition (MMT), characterized by an abrupt change in the magnetic quantities. MMTs are ubiquitous among the different heavy-fermion compounds, but due to the rich variety and complicated structure of their phase diagrams, the true nature of the MMT remains unknown. In particular, two competing scenarios are under consideration. The localization scenario proposes that the itinerant f electrons suddenly localize at the MMT, and the heavy-fermion state disappears at that point. An alternative scenario is given by a continuous evolution of the Fermi surface, in which the localization of the f electrons is not tied to the MMT.

Experimental results indicate the existence of MMTs in CeRu_2Si_2 and YbRh_2Si_2 , which have been attributed to the localization of the f electrons.^{4,5} Recent experiments on CeRu_2Si_2 , however, suggest that the localization scenario might not be appropriate.⁶ This was already pointed out in Ref. 7, in which static magnetization measurements ruled out the possibility of a first-order phase transition, at odds with the existent de Haas–van Alphen measurements.⁵ On the ba-

sis of Hall effect and magnetoresistance measurements, the authors of Ref. 6 proposed that the MMT anomalies result from a continuous evolution of the Fermi surface in which the spin-split sheet corresponding to the heaviest electrons shrinks to a point.

This paper elaborates on the continuous scenario. We argue that the underlying phenomenology is the systematic descent of the spin up quasiparticle band with applied field. The MMT corresponds to the point at which the entire spin up band drops below the chemical potential, and only at much higher fields do the f electrons localize. A common argument in favor of the localization scenario is that a sharp drop in γ , the linear coefficient of the specific heat, is always observed at the MMT. What renders this interpretation unconvincing is that the value of γ above the MMT is too large,^{4,8} as is the residual magnetic susceptibility.⁴ A better picture is that as the field is ramped up, the mass enhancement factor of the spin up quasiparticles increases, while that of the spin down decreases.^{9–11} At the MMT, the lower spin up band is completely filled, and the heaviest quasiparticles drop out of all thermodynamic quantities: the system goes from having a spin up Fermi surface of very heavy particles and a spin down surface of moderately heavy particles to having only the latter.

We address the theoretical aspects of such a transition from a mean-field point of view. Our approach goes well beyond the conventional c - f hybridization scheme in that it treats *all* the relevant competing interaction channels; it includes both singlet and triplet pairing and allows for spontaneous ferromagnetism. The particular compounds mentioned above are amenable to this kind of analysis because they are largely paramagnetic: they do not exhibit superconductivity, and antiferromagnetic ordering is suppressed by very small values of an applied external magnetic field. As to the overall reliability of the mean-field approach, comparison with dynamical mean-field simulations confirms that quantum fluctuations do not qualitatively change the behavior in the range of field strengths that are of interest for the MMT.¹²

The starting point for our analysis is the periodic Anderson model¹³ augmented by a Zeeman term. In the limit of infinite on-site repulsion, a Schrieffer–Wolf transformation maps the Hamiltonian to a model of conduction electrons coupled to an array of localized magnetic impurities,

$$\hat{H} = -t \sum_{\langle ij \rangle} (c_i^\dagger c_j + c_j^\dagger c_i) + \sum_i [J \hat{\mathbf{s}}_i \cdot \hat{\mathbf{S}}_i - \mu_B \mathbf{B} \cdot (g_c \hat{\mathbf{s}}_i + g_f \hat{\mathbf{S}}_i)]. \quad (1)$$

Here, $c_i^\dagger = (c_{i1}^\dagger, c_{i2}^\dagger)$ is the creation operator for the conduction electrons and $\hat{\mathbf{s}}_i = \frac{1}{2} c_i^\dagger \boldsymbol{\sigma} c_i$ is the operator that measures their local spin density. $\hat{\mathbf{S}}_i$ is the impurity pseudospin at site i . It, too, has an underlying fermion representation, $\hat{\mathbf{S}}_i = \frac{1}{2} f_i^\dagger \boldsymbol{\sigma} f_i$, but the infinite on-site repulsion suppresses all charge fluctuations, i.e., $f_i^\dagger f_i = 1$. The spinor components of f refer to the appropriate Kramers doublet: the degeneracy of the physical f electrons is effectively reduced to 2 by strong spin-orbit coupling and crystal field effects.¹⁴ For Ce and Yb, these are the doublets of the $4f^1$ and $4f^{13}$ atomic configurations.

In Eq. (1), Landé g factors have been introduced to allow for differential coupling of the c and f electrons to the applied field \mathbf{B} . (In what follows, we set the Bohr magneton $\mu_B = 1$.) The factor g_f , in particular, is highly nontrivial and depends on the details of the f -electron environment. In general, such moments are partially quenched,¹⁵ and simple estimates suggest that semirealistic values are in the range $1 \lesssim g_f \lesssim 1.5$ (see, e.g., Refs. 16 and 17), while $g_c \approx 2$. In particular, Ce^{3+} ($J=5/2$, $L=3$, $S=1/2$) has $g_f=7/6$ and Yb^{3+} ($J=7/2$ ($J=5/2$, $L=3$, $S=1/2$)) has $g_f=8/7$. The value of g_f may also have some field dependence,¹⁶ but this effect is weak enough to ignore.

Some authors have worked in the limit $g_c=0$ so that the field couples only to the impurity spin and not at all to the conduction electrons,^{18–23} but we do not believe that this is the correct starting point. A more common assumption is to set the two g factors equal.^{24–27} This choice, however, is a somewhat artificial limit²⁸ and, at the mean-field level, leads to a nongeneric ($g_c=g_f$ is a special tuning) magnetization plateau of width equal to the zero-field Kondo energy.^{9,12}

We do not attempt to model the anisotropy of g (it is, in principle, a tensor²⁹) by introducing explicit crystal field terms into the Hamiltonian.³⁰ We disregard the fact that metamagnetism appears when the field is applied parallel to an easy axis (the tetragonal c axis³¹). Another simplification in our model is that we do not consider the Ruderman–Kittel–Kasuya–Yosida (RKKY) interaction and, therefore, it is valid for paramagnetic ground states in which long range magnetic correlations are absent. Neglecting the RKKY interaction in our case is *a priori* justified since we are interested in the high external magnetic field regime.

In the next section, we present the mean-field construction for this Hamiltonian and derive the self-consistent equations that determine the mean-field parameters. We show that the mean field must include separate hybridization parameters in the spin up and spin down channels and a Weiss molecular field in order for the model to capture all the observed qualitative features of the system. Results from solving for the parameters are presented in Sec. III. In particular, we show

the evolution of the Kondo gap, mass enhancement factor, magnetization, and susceptibility of the system for increasing external magnetic field, and we sketch the phase diagram predicted by the model. We discuss our results in Sec. IV and provide a summary of our principal results in Sec. V. Some details of the calculations are relegated to the appendixes.

II. MEAN-FIELD APPROACH

A hybridization mean-field treatment of the KLM Hamiltonian was presented in Ref. 9 based on a decomposition in terms of the operators $\hat{\chi}^\mu = \frac{1}{\sqrt{2}} f_i^\dagger \sigma^\mu c$. The index μ ranges over 0, 1, 2, 3; in this notation, σ^0 is the 2×2 identity matrix and $\sigma^1, \sigma^2, \sigma^3$ are the Pauli matrices. These operators are complete ($\sum_\mu \chi^\mu \chi^\mu = 1$) in the $\frac{1}{2} \otimes \frac{1}{2} = 0 \oplus 1$ spin sectors and are introduced so that the exchange interaction can be explicitly broken up into singlet and triplet components,

$$\frac{1}{4} c^\dagger \boldsymbol{\sigma} c \cdot f_i^\dagger \boldsymbol{\sigma} f_i = -\frac{3}{4} \hat{\chi}^{0\dagger} \hat{\chi}^0 + \frac{1}{4} \hat{\chi}^\dagger \cdot \hat{\chi}. \quad (2)$$

Here, the three triplet components are represented using the vector notation $\hat{\chi}^\mu = (\hat{\chi}^0, \hat{\chi})$.

In the usual way, the right-hand side of Eq. (2) can be approximated by

$$\sum_\mu \left(\frac{1}{4} - \delta^{\mu 0} \right) (\chi^{\mu\dagger} \langle \chi^\mu \rangle - \langle \chi^\mu \rangle^* \chi^\mu - |\langle \chi^\mu \rangle|^2). \quad (3)$$

In zero field, it is customary to assume that only the singlet amplitude condenses ($\langle \hat{\chi}^0 \rangle \neq 0$ and $\langle \hat{\chi} \rangle = 0$). This gives rise to the conventional heavy-fermion state. At nonzero field, however, it is appropriate to consider the possibility of a nonzero *triplet* hybridization. For convenience, we introduce a spin-dependent hybridization energy,

$$V^0 = \frac{3J}{4\sqrt{2}} \langle \hat{\chi}^0 \rangle, \quad V^3 = \frac{J}{4\sqrt{2}} \langle \hat{\chi}^3 \rangle, \\ V_+ = V^0 - V^3, \quad V_- = V^0 + V^3. \quad (4)$$

These definitions are consistent with an applied magnetic field $\mathbf{B} = (0, 0, B)$ directed along the axis of spin quantization. Then, Eq. (3), the decomposition in the pairing channel, can be expressed as

$$J \hat{\mathbf{s}} \cdot \hat{\mathbf{S}} \xrightarrow{\text{pair}} -V^0 f_i^\dagger c - V^0 c^\dagger f_i + \frac{8|V^0|^2}{3J} + V^3 f_i^\dagger \sigma^3 c + V^3 c^\dagger \sigma^3 f_i \\ - \frac{8|V^3|^2}{J}. \quad (5)$$

The triplet hybridization, which to our knowledge has never been included in any mean-field treatment, plays an important role in the vicinity of the metamagnetic transition. Admitting the possibility of $V_\uparrow \neq V_\downarrow$ makes our theory compatible with the quasiparticle interpretation of the Gutzwiller approach.³²

We also decompose the Kondo interaction in the magnetic channel. That is,

$$\hat{\mathbf{S}} \cdot \hat{\mathbf{S}} \rightarrow \hat{\mathbf{S}}^{\text{mag}} \cdot \mathbf{m}_f + \mathbf{m}_c \cdot \hat{\mathbf{S}} - \mathbf{m}_c \cdot \mathbf{m}_f, \quad (6)$$

where $\mathbf{m}_c = \langle \hat{\mathbf{S}} \rangle$ and $\mathbf{m}_f = \langle \hat{\mathbf{S}} \rangle$. This sets up a Weiss molecular field, whereby every c electron feels the counterpolarizing effect of its local f partner, and vice versa. Such a contribution is necessary to reproduce the observed diamagnetism of the c electrons, which initially cant away from the applied field.^{26,27}

Summing the contributions of Eqs. (5) and (6) yields a complete mean-field Hamiltonian,

$$\begin{aligned} \hat{H}_{\text{MF}} = & -t \sum_{\langle ij \rangle} (c_i^\dagger c_j + c_j^\dagger c_i) - \sum_{is} (V_s c_{is}^\dagger f_{is} + V_s^* f_{is}^\dagger c_{is}) \\ & - \sum_{is} \sum_{a=c,f} a_{is}^\dagger a_{is} \left[\mu_a + \frac{s}{2} (g_a B - m_{\bar{a}} J) \right] + N \mathcal{F}_0. \end{aligned} \quad (7)$$

The indices i, j run over the lattice sites, N is the total number of sites, and $s = \pm 1$ corresponds to spins up and down. The bar indicates $\bar{a} = f$ (c) if $a = c$ (f). The overall constant is given by

$$\mathcal{F}_0 = \frac{4}{3J} (4V_+ V_- - V_+^2 - V_-^2) - J m_c m_f. \quad (8)$$

Note that we have introduced chemical potentials μ_c and μ_f in order to control the occupation of the c and f electrons; the constraints $\langle f_{i\uparrow}^\dagger f_{i\uparrow} \rangle = n_f \equiv 1$ and $\langle c_{i\uparrow}^\dagger c_{i\uparrow} \rangle = n_c$ are imposed on average. This mean-field decomposition is justified by a variational argument, detailed in Appendix A, which uniquely determines the numerical prefactors appearing in Eq. (8).

The mean-field Hamiltonian can then be written in Fourier space as

$$H_{\text{MF}} = \sum_{\mathbf{k}s} \begin{pmatrix} c_{\mathbf{k}s}^\dagger & f_{\mathbf{k}s}^\dagger \end{pmatrix} M_{\mathbf{k}s} \begin{pmatrix} c_{\mathbf{k}s} \\ f_{\mathbf{k}s} \end{pmatrix} + N \mathcal{F}_0, \quad (9)$$

with coefficient matrix

$$M_{\mathbf{k}s} = \begin{pmatrix} \epsilon_{\mathbf{k}} - \mu_c - \frac{s}{2} g_c B_c & -V_s \\ -V_s & -\mu_f - \frac{s}{2} g_f B_f \end{pmatrix}. \quad (10)$$

Here, $\epsilon_{\mathbf{k}}$ is the dispersion relation of the bare c electrons and $B_f = B - J m_c / g_f$, $B_c = B - J m_f / g_c$ are self-consistent Weiss fields. Note that the effective field felt by an a electron ($a = c, f$) differs considerably from the applied field when J is large and g_a is small.

The eigenvalues of $M_{\mathbf{k}s}$ are $E_{\mathbf{k}s}^n = I_{\mathbf{k}s}^n - \mu_f - \frac{s}{2} g_f B_f$, where $n = \pm 1$ is a quasiparticle band index and we have defined

$$I_{\mathbf{k}s}^n = \frac{1}{2} [\epsilon_{\mathbf{k}} - b_s + n \sqrt{(\epsilon_{\mathbf{k}} - b_s)^2 + 4V_s^2}], \quad (11)$$

with $b_s = b + (s/2)(g_c B_c - g_f B_f)$ and $b = \mu_c - \mu_f$. b is the chemical energy for transmuting c electrons into f electrons; it becomes increasingly important away from half filling.

In terms of the free energy $\mathcal{F} = \mathcal{F}_0 - \frac{1}{N\beta} \sum_{\mathbf{k}ns} \ln(1 + e^{-\beta E_{\mathbf{k}s}^n})$, the mean-field values are determined by solving the following system of equations:

$$\begin{aligned} -\frac{\partial \mathcal{F}}{\partial \mu_c} = n_c, \quad -\frac{1}{g_c} \frac{\partial \mathcal{F}}{\partial B_c} = m_c, \quad -\frac{\partial \mathcal{F}}{\partial V_-} = 0, \\ -\frac{\partial \mathcal{F}}{\partial \mu_f} = n_f, \quad -\frac{1}{g_f} \frac{\partial \mathcal{F}}{\partial B_f} = m_f, \quad -\frac{\partial \mathcal{F}}{\partial V_+} = 0. \end{aligned} \quad (12)$$

It is understood that

$$\begin{aligned} n_{c\uparrow} + n_{c\downarrow} = n_c, \quad n_{f\uparrow} + n_{f\downarrow} = n_f, \\ n_{c\uparrow} - n_{c\downarrow} = 2m_c, \quad n_{f\uparrow} - n_{f\downarrow} = 2m_f. \end{aligned} \quad (13)$$

Equation (12) can be translated to the continuum by defining $D_s(\omega) = \sum_{\mathbf{k}n} \delta(\omega - I_{\mathbf{k}s}^n)$, a density of states (DOS) shifted with respect to the true energy zero by $\mu_{fs} \equiv \mu_f + \frac{s}{2} g_f B_f$. Here, we can now follow the method described in Ref. 9, extending it to take the spin dependence into account. The result is as follows. If we assume that the bare conduction-electron DOS has the form

$$\sum_{\mathbf{k}} \delta(\omega - \epsilon_{\mathbf{k}}) = \phi(\omega) \theta(W^2 - 4\omega^2), \quad (14)$$

where $\phi(\omega)$ describes the spectral line shape and the Heaviside function θ demarcates the band edges at $-W/2$ and $W/2$, then the renormalized c -electron DOS is

$$D_s^c(\omega) = \phi \left(\omega - \frac{V_s^2}{\omega} + b_s \right) \sum_{l=1}^4 \theta(\omega - \omega_{ls}), \quad (15)$$

where the edges of the quasiparticle dispersion bands are now given by the expressions

$$\begin{aligned} \omega_{1s} &= -\frac{1}{4} \sqrt{(W + 2b_s)^2 + (4V_s)^2} - \frac{1}{4} (W + 2b_s), \\ \omega_{2s} &= -\frac{1}{4} \sqrt{(W - 2b_s)^2 + (4V_s)^2} + \frac{1}{4} (W - 2b_s), \\ \omega_{3s} &= +\frac{1}{4} \sqrt{(W + 2b_s)^2 + (4V_s)^2} - \frac{1}{4} (W + 2b_s), \\ \omega_{4s} &= +\frac{1}{4} \sqrt{(W - 2b_s)^2 + (4V_s)^2} + \frac{1}{4} (W - 2b_s). \end{aligned} \quad (16)$$

The total quasiparticle DOS is given by

$$D_s = D_s^c(\omega) + D_s^f(\omega) \quad \text{with} \quad D_s^f(\omega) = \frac{V_s^2}{\omega^2} D_s^c(\omega). \quad (17)$$

The Kondo gap depends on spin and is given by $\Delta_{Ks} = \omega_{3s} - \omega_{2s}$. It is straightforward to see that Δ_{Ks} collapses to zero when $V_s = 0$ and, therefore, it can be thought of as an alternative order parameter for the heavy-fermion state.

One finds that Eq. (12) is equivalent to (for each of $a = c, f$)

$$\begin{aligned}
 \sum_s \int d\omega f(\omega - \mu_{fs}) D_s^a(\omega) &= n_a, \\
 \sum_s \int d\omega f(\omega - \mu_{fs}) D_s^a(\omega) &= n_{a\uparrow} - n_{a\downarrow}, \\
 \frac{3J}{4} \int d\omega f(\omega - \mu_{fs}) \frac{D_s^c(\omega)}{\omega} &= 1 - \frac{2V_{-s}}{V_s}, \quad (18)
 \end{aligned}$$

where $f(\omega)$ denotes the Fermi function. In the special case of a flat c -electron spectrum $\phi=1/W$ and zero temperature $f(\omega - \mu_{fs}) \rightarrow \theta(\mu_{fs} - \omega)$, these integral equations have a closed form^{9,33} and thus can be solved efficiently everywhere in the J, B, n_c parameter space.

For $B > 0$, the important issue is where μ_{f+} sits with respect to the band edges. There are six possibilities:

(I)

$$\omega_{1-} < \mu_{f-} < \omega_{2-},$$

$$\omega_{1+} < \mu_{f+} < \omega_{2+}.$$

(II)

$$\omega_{1-} < \mu_{f-} < \omega_{2-},$$

$$\omega_{2+} < \mu_{f+} < \omega_{3+}.$$

(III)

$$\omega_{1-} < \mu_{f-} < \omega_{2-},$$

$$\omega_{3+} < \mu_{f+} < \omega_{4+}.$$

(IV)

$$\omega_{2-} < \mu_{f-} < \omega_{3-},$$

$$\omega_{2+} < \mu_{f+} < \omega_{3+}.$$

(V)

$$\omega_{2-} < \mu_{f-} < \omega_{3-},$$

$$\omega_{3+} < \mu_{f+} < \omega_{4+}.$$

(VI)

$$\omega_{3-} < \mu_{f-} < \omega_{4-},$$

$$\omega_{3+} < \mu_{f+} < \omega_{4+}.$$

In zero field, if the system is not spontaneously magnetic, we have a situation where $\mu_{f+} = \mu_{f-}$ sits either inside the lower hybridized bands ($0 < n_c < 1$) or inside the upper hybridized bands ($1 < n_c < 2$). We will restrict our attention to the case of less than half filling. (If the bare band structure is symmetric, then the two cases are equivalent.) When the external magnetic field is turned on, μ_{f-} will descend and μ_{f+} will ascend. For small fields ($B \ll \Delta_{Ks}$), the chemical potential of the spin up quasiparticles will still sit below the upper edge of the lower band ($\mu_{fs} < \omega_{2s}$). At larger fields, we have

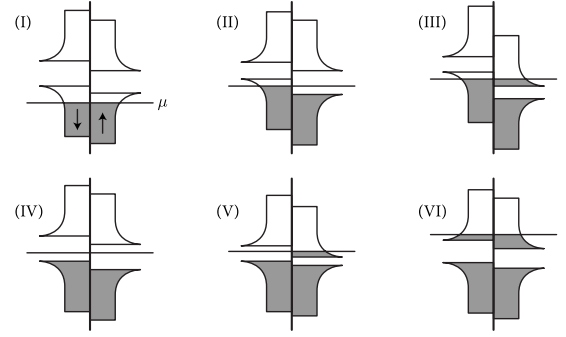


FIG. 1. The six possible placements of the bands with respect to the chemical potential. Cases (I) and (II) occur for $0 < n_c < 1$ and cases (V) and (VI) for $1 < n_c < 2$. Case (IV) occurs for the $n_c = 1$ Kondo insulator. We find that the controversial case (III) never occurs: it either has no solution or a solution that is energetically unfavorable.

to account for the possibility of μ_{f+} moving into the hybridization gap or into the upper quasiparticle band (positions II and III in Fig. 1). All of these possibilities have to be solved for, along with the $V_s = 0$ case, with the true ground state determined by energy considerations.

Some authors have ascribed the metamagnetic transition to a regime II \rightarrow III crossover^{19,28,34} or even to a direct regime I \rightarrow III transition.³⁵ Our model predicts, however, that the origins of metamagnetism lie in the smooth crossover from regime I to II. What we find is that at some field B^* , μ_{f+} moves smoothly into the gap so that μ_{f+} is replaced by ω_{2+} in the upper limits of the integrals in Eq. (18). Hence, the only explicit magnetic field dependence in the system of equations comes through $\mu_{f-} = m_f - \frac{1}{2} g_f B_f$. μ_{f-} itself becomes field independent ($\mu_{f-} = \text{const} + \frac{1}{2} g_f B_f$) and all the quantities that depend on it become locked at the values obtained at B^* . In the special case of $g_c = g_f$, $B = B^*$ marks the sudden collapse of the magnetic susceptibility to zero and the beginning of a large magnetic plateau. For general $g_c \neq g_f$, we instead see the susceptibility jump to a lower but nonzero value; the magnetization changes slope and becomes perfectly linear for $B > B^*$.

The crossover to the “locked” regime II is determined by the balance of the free energies evaluated at the two sets of solutions, if existing. The free energy density for the heavy-fermion state can be calculated from its expression in the continuum,

$$\mathcal{F} = \mathcal{F}_0 - \frac{1}{\beta} \sum_s \int d\omega D_s(\omega) \ln[1 + e^{-\beta(\omega - \mu_{fs})}]. \quad (19)$$

Using $\mathcal{F} = \partial(\beta\mathcal{F}) / \partial\beta$ and the self-consistent equations for V_s , we can obtain the functional expression for $\mathcal{F}(\mu_c, \mu_f, B)$ within the different regimes. For example, in regime I,

$$\begin{aligned}
 \mathcal{F}_I = & -Jm_c m_f - g_f B_f (m_c + m_f) - \mu_f (n_c + n_f) \\
 & + \frac{1}{2W} \sum_s (\mu_{fs}^2 - \omega_{1s}^2). \quad (20)
 \end{aligned}$$

From the definition of the free energy, $\mathcal{F}(\mu_c, \mu_f, B)$

$=\mathcal{U}(n_c, n_f, m) - Bm - \mu_c n_c - \mu_f n_f$, we can also compute the Gibbs free energy, $\mathcal{G}(n_c, n_f, B) = \mathcal{U} - Bm$. Here, we have written the total magnetization $m = g_c m_c + g_f m_f$, and it is understood that we are working at zero temperature. It is convenient to introduce a quantity x , defined by $n_c = 1 - x$, that measures the deviation from half filling. Since $n_f = 1$ is fixed, we can write $\mathcal{G}(x, B) = \mathcal{F}(\mu_c, \mu_f, B) + \mu_c(1 - x) + \mu_f$. For regime I, we find

$$\mathcal{G}_I = b(1 - x) - Bg_f(m_c + m_f) + Jm_c^2 + \frac{1}{2W} \sum_s (\mu_{f_s}^2 - \omega_{1s}^2). \quad (21)$$

The free energy for the locked regime II is obtained by substituting $\mu_{f_+} \rightarrow \omega_{2+}$ in Eqs. (20) and (21).

In the limit $V_+ = V_-$ and $B = B_c = B_f$, which corresponds to the simpler mean-field theory described in Ref. 9, this reduces to

$$\mathcal{G} = \frac{1}{W} \left(\mu_{f_+}^2 + \frac{1}{4} B^2 - \omega_1^2 \right) - B(m_c + m_f) + b(1 - x). \quad (22)$$

The heavy-fermion state will collapse when the free energy \mathcal{G} of the heavy-fermion (in phase I, II, or III) is greater than either the free energy \mathcal{G}_{PM} of a normal paramagnetic metallic state or the free energy \mathcal{G}_{IF} of a conventional itinerant ferromagnet. This transition occurs at a critical field B^c such that either $\mathcal{G} = \mathcal{G}_{PM}$ or $\mathcal{G} = \mathcal{G}_{IF}$, whichever is smaller. The expressions for these energies are given in Appendix B, where we also present the criterion for determining which end state wins out.

III. RESULTS

The system of equations [Eq. (18)] was solved numerically by turning on adiabatically the external magnetic field B , for different values of the Kondo coupling J and filling factor x . A typical phase diagram obtained with our model is shown in the bottom plot of Fig. 2 for a particular value of the exchange coupling J and as a function of the filling factor x . We see that there is always a magnetic field $B^* < B^c$ for which the system enters the locked state, regime II. As we discussed in the previous section, B^* corresponds to the magnetic field for which $\mu_{f_+} = \omega_2$. Between B^* and B^c , μ_{f_+} is inside the gap and, as we discussed earlier, the set [Eq. (18)] has a field-independent solution. B^c is the critical magnetic field at which the heavy-fermion state is destroyed. From the diagram, we also see that the heavy-fermion state always collapses before regime III can be reached.

The top plot of Fig. 2 shows the behavior of B^* as a function of the filling factor x for different values of J . As the coupling J decreases, the heavy metal phase is constrained to smaller values of x . It is interesting to note that while the field B^c is a monotonic decreasing function of x , B^* has a dome shape and it is maximum for x at approximately the midpoint of the range for the regime I phase determined for each J . The behavior of B^c , which is not shown in this plot, is similar to the behavior depicted in the phase diagram for $J/W = 0.7$. It is important to remark that B^c is always at least

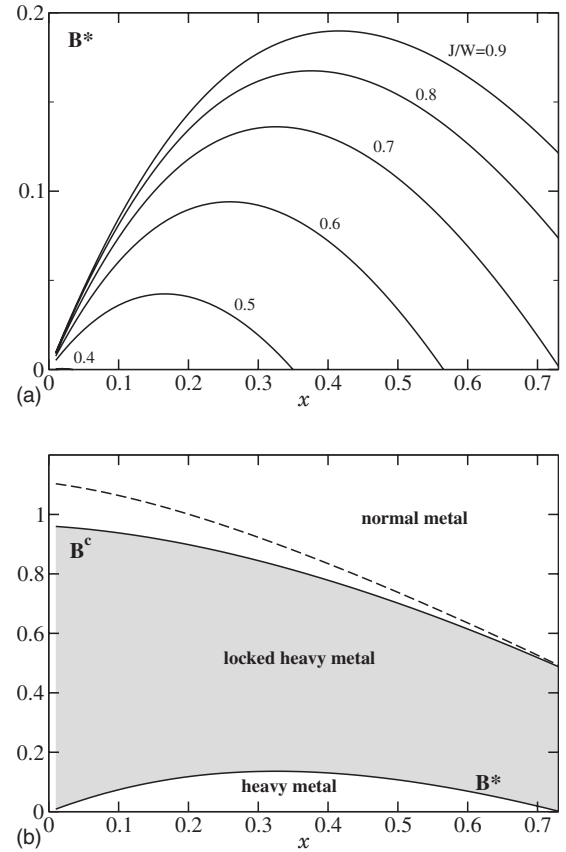


FIG. 2. (Top) The crossover field B^* at which μ_{f_+} moves into the hybridization gap is plotted in units of the zero-field gap as a function of the filling parameter x for various values of the Kondo coupling. We have chosen $g_c = 2$, $g_f = 8/7$. (Bottom) $J/W = 0.7$. B^* is the MMT and B^c is the critical field of the first-order transition back to the normal state. The dashed line marks the point at which μ_{f_+} would have entered the upper quasiparticle band if it had not been pre-empted by the destruction of the heavy state.

1 order of magnitude larger than B^* . To the right of the dome enclosing the regime I heavy metal, the system is already in the locked phase at $B = 0$, implying a spontaneous polarization. This can be related to the existence of strong ferromagnetic correlations at low n_c .^{33,36} It is known that a ferromagnetic state exists in the limit of a single conduction electron, $n_c \rightarrow 0^+$ ($x \rightarrow 1^-$).³⁷

By fixing both J and x , we can plot the total magnetization of the system, as shown in Fig. 3 for $J/W = 0.7$ and $x = 0.4$. The total magnetization is defined as $m = g_c m_c + g_f m_f$, m_c giving a diamagnetic contribution. We see that there is a strong nonlinear increase of the magnetization up to $B = B^*$. At this value of the external field, there is an abrupt change signaled by a kink, after which the magnetization is purely linear with the field. At larger values of the field (not shown in the figure), another change would be expected at $B = B^c$ due to the collapse of the heavy-fermion state. The inset of Fig. 3 shows the total susceptibility, which decreases in a nonlinear fashion up to B^* and then jumps down abruptly to a constant. These plots are in remarkable qualitative agreement with the magnetic behavior found recently for YbRh_2Si_2 , as can be seen by comparing with Ref. 4.

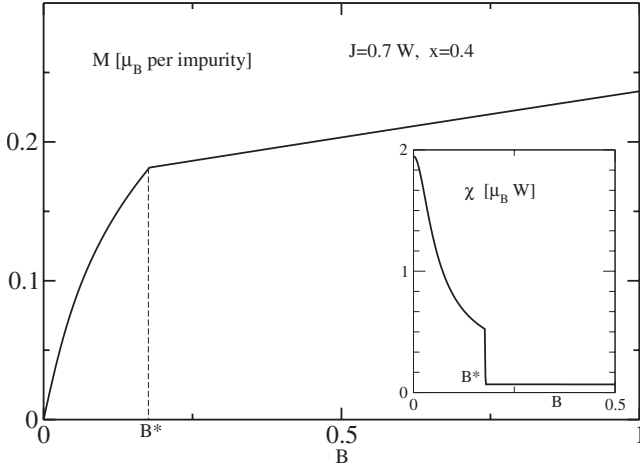


FIG. 3. (Main) Total magnetization of the system with $g_f=8/7$, $g_c=2$ for $J/W=0.7$ and filling factor $x=0.4$ as a function of the magnetic field in units of the zero-field gap. B^* is the MMT. The critical field B^c is out of the plot range. (Inset) Total susceptibility.

The mass enhancement of the quasiparticles can be computed via the expression $(M^*/M) = \partial I_{ks}^n / \partial \epsilon_{ks}$ evaluated at the Fermi surface, where M^* is the effective mass of the quasiparticles, while M is the mass given by the noninteracting bands. The result, again for $J/W=0.7$ and $x=0.4$, is shown in Fig. 4. As predicted, the effective mass of the spin up (down) band increases (decreases) with increasing field. For $B > B^*$, however, the spin up band becomes infinitely massive, while the spin down effective mass becomes roughly a constant. The inset of Fig. 4 shows the splitting of the Kondo gap due to the magnetic field.

The locked state can only be avoided if the heavy-fermion state collapses before the locked state is reached. This can be engineered for a small range of the parameters J and x , if we

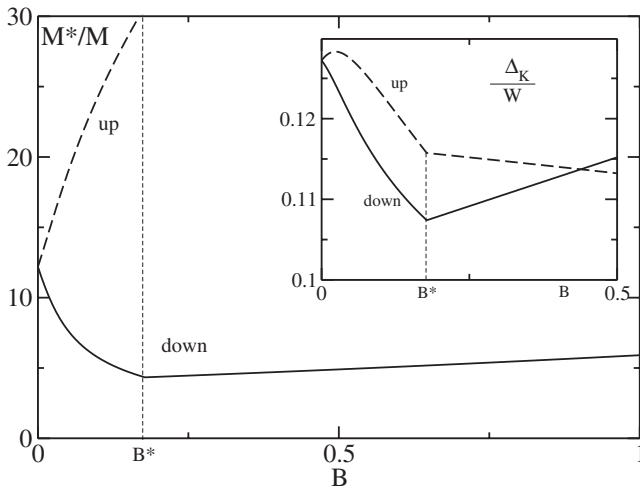


FIG. 4. (Main) Mass enhancement factor for spin up (dashed) and spin down (solid) bands with $g_f=8/7$, $g_c=2$ for $J/W=0.7$ and filling factor $x=0.4$ as a function of the magnetic field in units of the zero-field gap. B^* is the MMT. The critical field B^c is out of the plot range. (Inset) Kondo gap for spin up (dashed) and spin down (solid) bands.

assume $g_f < 1$. This assumption, however, is not justified by our simple estimates of g_f . Also, the very constrained range of parameters for which this behavior is obtained within our model would imply a high degree of fine tuning.

IV. DISCUSSION

Our model seems to capture qualitatively the physics behind the MMT of YbRh_2Si_2 , indicating that the MMT is due to the crossover in which the spin up band ceases to participate in the heavy-fermion state. Meanwhile, the spin down band contributes with a moderately large effective mass. The corresponding magnetic susceptibility is a moderately large constant value, as observed in YbRh_2Si_2 .⁴ The collapse of the heavy-fermion phase is reserved for much higher fields, at least 1 order of magnitude larger than the MMT field. This is in agreement with observations for CeRu_2Si_2 , which locate the MMT at approximately 10 T, while the complete suppression of the heavy-fermion state is not realized before fields on the order of 100 T.⁸ We emphasize that the magnetic field strength required to polarize the quasiparticles of the renormalized heavy-fermion bands is not on the order of the bandwidth, as is the case in the noninteracting ($J=0$) system. This is so due to the formation of hole pockets at the top of the lower band, with characteristic energies of the order of the Kondo temperature, which are inherent to the hybridization process.³⁸

There is a qualitative difference between the MMT transition of YbRh_2Si_2 and the one of CeRu_2Si_2 . While for the Yb compound the magnetization presents a rather smooth kink and the magnetic susceptibility jumps down, for the Ce compound, there is a pronounced peak in the susceptibility at the MMT. According to our model, there is no such peak at B^* , although a peak would be observed in the susceptibility at B^c . However this would imply that the heavy-fermion state is destroyed, and the remnant heavy-fermion behavior would then be unexplained. This apparent contradiction was previously pointed out in Ref. 6. A very similar behavior to that of CeRu_2Si_2 is observed for another heavy-fermion compound, UPt_3 .³⁹ Moreover, a spin-split surface was observed in UPt_3 , with one of the components surviving with high mass after the MMT.⁴⁰ The peak in the susceptibility in these compounds is usually attributed to enhanced antiferromagnetic fluctuations^{4,6,8,39} and, therefore, it would be reasonable to expect that RKKY interactions, which are neglected in our model, play an important role at the MMT of these materials.

In order to compare quantitatively with the experimental data, we need to fix the free parameters: the Kondo coupling J , the filling factor x , and the bandwidth W . This is not trivial since these are noninteracting parameters and, therefore, their true value is unknown. This is also true for the gyromagnetic factors g_c and g_f which we will take as in the previous section, $g_f=8/7$, $g_c=2$. We begin by fixing B^* , by imposing that it coincides with the MMT. Therefore, we identify $B^* \approx 10$ T, as a reasonable order of magnitude suggested by the available experimental data.^{4,5} Choosing a value for the noninteracting bandwidth W restricts the range of x and J . For $W \approx 1$ eV $\approx 10^4$ K $\approx 10^4$ T, we find that $B^*/W \approx 10^{-3}$. To fix the values of J and x , we are guided the phase

diagrams depicted in Fig. 2. For attaining such small values of B^*/W , we see that x has to be either small or close in value to J/W . Since the fraction of conduction electrons controls the magnetization, bigger x will result in higher values of magnetization. Choosing $x=0.69$ for $J/W=0.7$ gives a total magnetization of $m \approx 0.5\mu_B$ per impurity at the MMT, which is of the same order of magnitude as the one observed for YbRh_2Si_2 . However, the residual susceptibility after the MMT is 2 orders of magnitude less than the experimentally observed, and the Kondo gap is approximately 100 K, which is four times bigger than the Kondo temperature for the material.⁴¹

However, for $x=0.4$ and $J/W=0.7$, we get a Kondo gap of ≈ 10 K, a magnetization of $m \approx 0.2\mu_B$ per impurity at the MMT, and a susceptibility of $\approx 0.01\mu_B/\text{T}$ per impurity, which are all of the order of magnitude of the experimental data. The drawback assumes a noninteracting bandwidth of $W \approx 10^{-2}$ eV, which seems unphysical. Nonetheless, this kind of scale problem seems to be ubiquitous among the various Kondo lattice models, see, for example, Refs. 24 and 30.

V. SUMMARY

We have studied the Kondo lattice model away from half filling in an external magnetic field within a mean-field approach. Our mean-field Hamiltonian is a generalization to high magnetic fields of the one presented in Ref. 9. This generalization is twofold: we allow for hybridization both in the singlet and triplet channels, plus we consider the self-consistent Weiss fields in the magnetic channel. We also work in the general case in which the c and f electrons couple differently to the magnetic field, introducing two different gyromagnetic factors g_c and g_f . This results in a spin-split very massive quasiparticle Fermi surface, which evolves with the magnetic field.

We showed that the self-consistent solution of this model exhibits a crossover followed by a first-order transition. At a moderate field of the order of the Kondo gap at zero field, which we called B^* , the spin up band enters the gap and its Fermi surface shrinks to a point, consequently disappearing from the problem. The spin down band, however, remains hybridized and mass enhanced. This behavior is signaled by a kink in the magnetization, which changes from a nonlinear dependence for fields smaller than B^* to a purely linear one after the crossover. The magnetic susceptibility shows an abrupt jump at B^* and afterward it is a constant. At a higher field B^c , approximately 1 order of magnitude greater than B^* , the heavy-fermion state collapses completely. The intermediate region between B^* and B^c we have dubbed the locked phase since the solution of the model is (explicitly) independent of the external field. Our results were obtained in the limit of zero temperature. As usual, it is expected that a finite temperature will have a smearing effect on the signatures of the MMT, and the kink in the magnetization will eventually disappear.⁴ The relevant energy scale is the difference between the Fermi energy and the top of the lower hybridized band.

These results are in excellent qualitative agreement with the MMT shown by the heavy-fermion compound YbRh_2Si_2 ,

which had been previously attributed to the localization of the f electrons.⁴ Quantitative agreement can also be achieved but at the expense of assuming unphysically small values for the noninteracting bandwidth W . Nonetheless, this does not imply any internal inconsistency in our model since W is always the biggest energy scale of the model.

The existence of the locked phase is guaranteed when we use simple estimates of the gyromagnetic factors, based on crystal field splitting arguments. If we choose $g_f < 1$, there is a very small range of the parameters x and J for which $B^c < B^*$. In this case, the heavy-fermion state is destroyed before the locked state is attained and, hence, there is no residual heavy-fermion behavior after the transition. g_c , in turn, controls the diamagnetic contribution to the total magnetization. We find that regime III, in which the upper band starts being filled by the spin up quasiparticles, never occurs because the heavy-fermion state always collapses before reaching this regime.

ACKNOWLEDGMENT

S.V.K. would like to thank C. Y. Hou, A. Rahmanisison, S. Rowley, and V. M. Pereira for enlightening discussions.

APPENDIX A: MEAN-FIELD DECOMPOSITION

The mean-field Hamiltonian is diagonalized by the unitary transformation

$$U = \begin{pmatrix} U^{c+} & U^{c-} \\ U^{f+} & U^{f-} \end{pmatrix} = \begin{pmatrix} \frac{-I^+}{\sqrt{(I^+)^2 + V^2}} & \frac{-I^-}{\sqrt{(I^-)^2 + V^2}} \\ V & V \\ \frac{V}{\sqrt{(I^+)^2 + V^2}} & \frac{V}{\sqrt{(I^-)^2 + V^2}} \end{pmatrix}.$$

We have suppressed the wave vector and spin-projection dependence, which arises since $U_{\mathbf{k}s}^{an}$ is an explicit function of $I_{\mathbf{k}s}^n$ [Eq. (11)]. The quasiparticles of the mean-field Hamiltonian are an admixture of the two fermion species, $\alpha_{\mathbf{k}s}^n = \sum_{a=c,f} a_{\mathbf{k}s} U_{\mathbf{k}s}^{an*}$, and describe the dynamics of the noninteracting system,

$$\begin{aligned} \hat{H}_0 &= \sum_{\mathbf{k}n s} E_{\mathbf{k}s}^n \alpha_{\mathbf{k}s}^{n\dagger} \alpha_{\mathbf{k}s}^n \\ &= \sum_{\mathbf{k}} [c_{\mathbf{k}}^\dagger (\epsilon_{\mathbf{k}} - \mu_c - sB_c/2) c_{\mathbf{k}} - f_{\mathbf{k}}^\dagger (\mu_f + sB_f/2) f_{\mathbf{k}} \\ &\quad - V_s (c_{\mathbf{k}s}^\dagger f_{\mathbf{k}s} + f_{\mathbf{k}s}^\dagger c_{\mathbf{k}})]. \end{aligned}$$

The complete Hamiltonian can be expressed as the sum $\hat{H} = \hat{H}_0 + \hat{H}_1$, where

$$\begin{aligned} \hat{H}_1 &= \sum_{\mathbf{k}} \left[V_s (c_{\mathbf{k}s}^\dagger f_{\mathbf{k}s} + f_{\mathbf{k}s}^\dagger c_{\mathbf{k}s}) - \frac{1}{2} (B - B_c) c_{\mathbf{k}}^\dagger \sigma^3 c_{\mathbf{k}} - \frac{1}{2} (B \right. \\ &\quad \left. - B_f) f_{\mathbf{k}}^\dagger \sigma^3 f_{\mathbf{k}} + \frac{J}{4} \sum_{\mathbf{q}, \mathbf{k}'} (c_{\mathbf{k}+\mathbf{q}}^\dagger \boldsymbol{\sigma} c_{\mathbf{k}}) \cdot (f_{\mathbf{k}'}^\dagger \boldsymbol{\sigma} f_{\mathbf{k}'+\mathbf{q}}) \right]. \quad (\text{A1}) \end{aligned}$$

If we take expectation values of the Hamiltonian in the ground state of \hat{H}_0 , we arrive at a variational energy \mathcal{U}

$=\langle\hat{H}\rangle=\sum_{\mathbf{k}n_s}E_{\mathbf{k}s}^n f_{\mathbf{k}s}^n+\langle\hat{H}_1\rangle$. Here, $f_{\mathbf{k}s}^n=\theta(-E_{\mathbf{k}s}^n)$ is the zero-temperature Fermi function.

In order to compute the expectation value $\langle\hat{H}_1\rangle$, we must substitute $c_{\mathbf{k}s}=\sum_{n=\pm}U_{\mathbf{k}s}^{cn}\alpha_{\mathbf{k}s}^n$ and $f_{\mathbf{k}s}=\sum_{n=\pm}U_{\mathbf{k}s}^{fn}\alpha_{\mathbf{k}s}^n$ into the various terms in Eq. (A1). For example, the four-body term $(c_{\mathbf{k}+\mathbf{q}}^\dagger\sigma c_{\mathbf{k}})\cdot(f_{\mathbf{k}'}^\dagger\sigma f_{\mathbf{k}'+\mathbf{q}})$ becomes

$$U_{\mathbf{k}+\mathbf{q},s}^{cn\dagger}U_{\mathbf{k},r}^{cm}U_{\mathbf{k}',r'}^{fn\dagger}U_{\mathbf{k}'+\mathbf{q},s'}^{fn'}\sigma_{sr}\cdot\sigma_{r's'}\alpha_{\mathbf{k}+\mathbf{q},s}^{n\dagger}\alpha_{\mathbf{k},r}^m\alpha_{\mathbf{k}',r'}^{m'\dagger}\alpha_{\mathbf{k}'+\mathbf{q},s'}^{n'}.$$

Expectation values of the quasiparticle operators obey Wick's theorem,

$$\begin{aligned}\langle\alpha_{\mathbf{k}+\mathbf{q},s}^{n\dagger}\alpha_{\mathbf{k},r}^m\alpha_{\mathbf{k}',r'}^{m'\dagger}\alpha_{\mathbf{k}'+\mathbf{q},s'}^{n'}\rangle &= f_{\mathbf{k}+\mathbf{q},s}^n(1-f_{\mathbf{k},r}^m)\delta_{ss'}^{nm'}\delta_{rr'}^{mm'}\delta_{\mathbf{k}\mathbf{k}'} \\ &+ f_{\mathbf{k},r}^m f_{\mathbf{k}',r'}^{n'}\delta_{sr}^{nm}\delta_{s'r'}^{m'n'}\delta_{\mathbf{q}0}\end{aligned}$$

Hence, using the identity $\sigma_{sr}\cdot\sigma_{r's'}=2\delta_{ss'}\delta_{rr'}-\delta_{sr}\delta_{s'r'}$, we find that the last term in Eq. (A1) is

$$\begin{aligned}\frac{1}{4}\sum_{sr}(2-\delta_{sr})\sum_{\mathbf{k}}U_{\mathbf{k}s}^{cn\dagger}U_{\mathbf{k},s}^{fn}\sum_{\mathbf{k}'}U_{\mathbf{k}'r}^{cm}U_{\mathbf{k}',r'}^{fn\dagger}(1-f_{\mathbf{k}',r}^m) \\ +\sum_{\mathbf{k}n_s}\frac{s}{2}U_{\mathbf{k}s}^{cn\dagger}U_{\mathbf{k},s}^{cn}\sum_{\mathbf{k}'s'n'}\frac{s'}{2}U_{\mathbf{k}'s'}^{fn\dagger}U_{\mathbf{k}',s'}^{fn'}f_{\mathbf{k}'s'}^{n'}.\end{aligned}$$

This result can be written compactly as

$$-\frac{1}{4}\sum_{sr}(2-\delta_{sr})\langle c_{\mathbf{k}s}^\dagger f_{\mathbf{k}s}\rangle\langle f_{\mathbf{k}',r}^\dagger c_{\mathbf{k}',r'}\rangle+\frac{1}{4}\langle c_{\mathbf{k}}^\dagger\sigma^3 c_{\mathbf{k}}\rangle\langle f_{\mathbf{k}}^\dagger\sigma^3 f_{\mathbf{k}}\rangle,$$

since the term $\sum_{\mathbf{k}n}U_{\mathbf{k}s}^{cn}U_{\mathbf{k}s}^{fn\dagger}$ can be shown to vanish identically,

$$-\frac{1}{W}\sum_s\int d\omega\frac{V_s}{\omega}=\sum_s\frac{V_s}{W}\log\left(\frac{\omega_{3s}\omega_{1s}}{\omega_{4s}\omega_{2s}}\right)\equiv 0.$$

Finally, the expectation value of Eq. (A1) is

$$\begin{aligned}\langle\hat{H}_1\rangle &= \sum_{\mathbf{k}}\left[\sum_s V_s\langle c_{\mathbf{k}s}^\dagger f_{\mathbf{k}s}+f_{\mathbf{k}s}^\dagger c_{\mathbf{k}s}\rangle-\frac{1}{2}(B-B_c)\langle c_{\mathbf{k}}^\dagger\sigma^3 c_{\mathbf{k}}\rangle\right. \\ &- \frac{1}{2}(B-B_f)\langle f_{\mathbf{k}}^\dagger\sigma^3 f_{\mathbf{k}}\rangle-\frac{J}{4}\sum_{sr\mathbf{k}'}(2-\delta_{sr})\langle c_{\mathbf{k}s}^\dagger f_{\mathbf{k}s}\rangle\langle f_{\mathbf{k}',r}^\dagger c_{\mathbf{k}',r'}\rangle \\ &\left. +\frac{J}{4}\langle c_{\mathbf{k}}^\dagger\sigma^3 c_{\mathbf{k}}\rangle\langle f_{\mathbf{k}}^\dagger\sigma^3 f_{\mathbf{k}}\rangle\right].\end{aligned}$$

We know that ultimately the hybridization and Weiss fields are going to behave as $Jm_c=Q(B-B_f)$, $Jm_f=Q(B-B_c)$, and $J\langle c_{\mathbf{k}s}^\dagger f_{\mathbf{k}s}\rangle=J\langle f_{\mathbf{k}s}^\dagger c_{\mathbf{k}s}\rangle=PV_s+\bar{P}V_{-s}$, where $m_c=\frac{1}{2}\langle c_{\mathbf{k}}^\dagger\sigma^3 c_{\mathbf{k}}\rangle$ and $m_f=\frac{1}{2}\langle f_{\mathbf{k}}^\dagger\sigma^3 f_{\mathbf{k}}\rangle$ and P , \bar{P} , and Q are unknown factors of proportionality. The extremal values are $P=-4/3$, $\bar{P}=8/3$, and $Q=1$, which lead to

$$\langle\hat{H}_1\rangle=\frac{8|V^0|^2}{3J}-\frac{8|V^3|^2}{J}-\frac{(B-B_c)(B-B_f)}{J}.$$

APPENDIX B: FREE ENERGY

1. Conventional paramagnetic metal

From Eq. (1), if we put the pairing channel to zero and assume $B_c=B_f=B$, we get

$$\mathcal{G}_{\text{PM}}=-\frac{W}{4}(1-x^2)-\frac{g_c^2 B^2}{4W}-\frac{g_f|B|}{2}+Jm_c m_f.$$

The corresponding magnetization is given by

$$m_c=\frac{g_c B}{2W}\quad\text{and}\quad m_f=\frac{1}{2}\text{sgn}(B).$$

2. Conventional itinerant ferromagnet

Again, we put the pairing channel to zero in Eq. (1) but this time we keep the Weiss fields defined by $g_c B_c=g_c B-Jm_f$ and $g_f B_f=g_f B-Jm_c$. The free energy takes the form

$$\mathcal{G}_{\text{IF}}=-\frac{W}{4}(1-x^2)-\frac{g_c^2 B_c^2}{4W}-\frac{g_f|B_f|}{2}-Jm_c m_f,$$

where the magnetization is given by $m_c=\frac{g_c B_c}{2W}$ and $m_f=\frac{1}{2}\text{sgn}(B_f)$. Hence,

$$\mathcal{G}_{\text{IF}}=-\frac{W}{4}(1-x^2)-\frac{g_c^2 B^2}{4W}-\frac{1}{2}\left(g_f-\frac{g_c J}{2W}\right)B\text{sgn}(B_f)-\frac{J^2}{16W}.$$

Clearly, the energy is a minimum when $\text{sgn}(B_f)=\text{sgn}(B)\text{sgn}\left(1-\frac{g_c J}{2g_f W}\right)$ and, therefore,

$$\mathcal{G}_{\text{IF}}=-\frac{W}{4}(1-x^2)-\frac{g_c^2 B^2}{4W}-\frac{1}{2}g_f|B|\left|1-\frac{g_c J}{2g_f W}\right|-\frac{J^2}{16W}.$$

The magnetization is then given by

$$m_c=-\frac{1}{B}\frac{\partial\mathcal{G}}{\partial g_c}=\text{sgn}(B)\left[\frac{g_c|B|}{2W}-\frac{J}{4W}\zeta\right],$$

$$m_f=-\frac{1}{B}\frac{\partial\mathcal{G}}{\partial g_f}=\frac{1}{2}\zeta\text{sgn}(B),$$

where $\zeta=\text{sgn}\left(1-\frac{g_c J}{2g_f W}\right)$. Notice that when $\zeta=1$, there is a line $|B|=J/2g_c$ at which m_c changes sign. There is no diamagnetic region when $\zeta=-1$.

The condition for the transition to be to an itinerant ferromagnet instead to a paramagnet is given by the condition $\mathcal{G}_{\text{IF}}<\mathcal{G}_{\text{PM}}$, which is satisfied for

$$|B|<\frac{J}{4(g_c-1)}\quad(\zeta=1),$$

$$|B|<\frac{J^2}{4[4g_f W-J(g_c+1)]}\quad(\zeta=-1).$$

- ¹J. M. Luttinger, *Phys. Rev.* **119**, 1153 (1960).
- ²D. M. Newns and N. Read, *Adv. Phys.* **36**, 799 (1987).
- ³G. R. Stewart, *Rev. Mod. Phys.* **56**, 755 (1984).
- ⁴Y. Tokiwa, P. Gegenwart, T. Radu, J. Ferstl, G. Sparn, C. Geibel, and F. Steglich, *Phys. Rev. Lett.* **94**, 226402 (2005).
- ⁵H. Aoki, S. Uji, A. K. Albessard, and Y. Onuki, *Phys. Rev. Lett.* **71**, 2110 (1993).
- ⁶R. Daou, C. Bergemann, and S. R. Julian, *Phys. Rev. Lett.* **96**, 026401 (2006).
- ⁷T. Sakakibara, T. Tayama, K. Matsuhira, H. Mitamura, H. Amit-suka, K. Maezawa, and Y. Onuki, *Phys. Rev. B* **51**, 12030 (1995).
- ⁸H. P. van der Meulen, A. de Visser, J. J. M. Franse, T. T. J. M. Berendschot, J. A. A. J. Perenboom, H. van Kempen, A. Lacerda, P. Lejay, and J. Flouquet, *Phys. Rev. B* **44**, 814 (1991).
- ⁹K. S. D. Beach, arXiv:cond-mat/0509778v1 (unpublished).
- ¹⁰J. Spałek and P. Gopalan, *Phys. Rev. Lett.* **64**, 2823 (1990); P. Korbel, J. Spałek, W. Wójcik, and M. Acquarone, *Phys. Rev. B* **52**, R2213 (1995).
- ¹¹Seiichiro Onari, Hiroshi Kontani, and Yukio Tanaka, *J. Phys. Soc. Jpn.* **77**, 023703 (2008).
- ¹²K. S. D. Beach and F. F. Assaad, arXiv:0802.1066v1 (unpublished).
- ¹³P. W. Anderson, *Phys. Rev.* **124**, 41 (1961).
- ¹⁴P. A. Lee, T. M. Rice, J. W. Serene, L. J. Sham, and J. W. Willkins, *Comments Condens. Matter Phys.* **12**, 99 (1986).
- ¹⁵Z. Zou and P. W. Anderson, *Phys. Rev. Lett.* **57**, 2073 (1986).
- ¹⁶R. Pietri, C. R. Rotundu, B. Anraka, B. C. Daniels, and K. Ingersent, *J. Appl. Phys.* **97**, 10A510 (2005).
- ¹⁷T. Izumi, Y. Imai, and T. Saso, *J. Phys. Soc. Jpn.* **76**, 084715 (2007).
- ¹⁸F. J. Ohkawa, *Solid State Commun.* **71**, 907 (1989).
- ¹⁹T. M. Hong and G. A. Gehring, *Phys. Rev. B* **46**, 231 (1992).
- ²⁰T. Saso and M. Itoh, *Phys. Rev. B* **53**, 6877 (1996).
- ²¹Y. Ono, *J. Phys. Soc. Jpn.* **65**, 19 (1996).
- ²²Y. Ono, *J. Phys. Soc. Jpn.* **67**, 2197 (1998).
- ²³H. Satoh and F. J. Ohkawa *Phys. Rev. B* **63**, 184401 (2001).
- ²⁴D. Meyer and W. Nolting, *Phys. Rev. B* **64**, 052402 (2001).
- ²⁵I. Milat, F. Assaad, and M. Sigrist, *Eur. Phys. J. B* **38**, 571 (2004).
- ²⁶K. S. D. Beach, P. A. Lee, and P. Monthoux, *Phys. Rev. Lett.* **92**, 026401 (2004).
- ²⁷T. Ohashi, A. Koga, S. I. Suga, and N. Kawakami, *Phys. Rev. B* **70**, 245104 (2004).
- ²⁸M. Nakano, *Phys. Rev. B* **44**, 10300 (1991).
- ²⁹J. Sichelschmidt, V. A. Ivanshin, J. Ferstl, C. Geibel, and F. Steglich, *Phys. Rev. Lett.* **91**, 156401 (2003).
- ³⁰R. Konno, *J. Phys.: Condens. Matter* **3**, 9915 (1991).
- ³¹L. Puech, J.-M. Mignot, O. Lejay, P. Haen, and J. Flouquet, *J. Low Temp. Phys.* **70**, 237 (1988).
- ³²A. M. Reynolds, D. M. Edwards, and A. C. Hewson, *J. Phys.: Condens. Matter* **4**, 7589 (1992).
- ³³C. Lacroix and M. Cyrot, *Phys. Rev. B* **20**, 1969 (1979).
- ³⁴T. M. Hong, *Phys. Rev. B* **46**, 13862 (1992).
- ³⁵D. M. Edwards and A. C. M. Green, *Z. Phys. B: Condens. Matter* **103**, 243 (1997).
- ³⁶K. Yamamoto and K. Ueda, *J. Phys. Soc. Jpn.* **59**, 3284 (1990).
- ³⁷M. Sigrist, H. Tsunetsugu, and K. Ueda, *Phys. Rev. Lett.* **67**, 2211 (1991).
- ³⁸J. D. Denlinger, G. H. Gweon, J. W. Allen, C. G. Olson, M. B. Maple, J. L. Sarrao, P. E. Armstrong, Z. Fisk, and H. Yamagami, *J. Electron Spectrosc. Relat. Phenom.* **117-118**, 347 (2001).
- ³⁹H. P. van der Meulen, Z. Tarnawski, A. de Visser, J. J. M. Franse, J. A. A. J. Perenboom, D. Althof, and H. van Kempen, *Phys. Rev. B* **41**, 9352 (1990).
- ⁴⁰S. R. Julian, P. A. A. Teunissen, and S. A. J. Wieggers, *Phys. Rev. B* **46**, 9821 (1992).
- ⁴¹P. Gegenwart, J. Custers, C. Geibel, K. Neumaier, T. Tayama, K. Tenya, O. Trovarelli, and F. Steglich, *Phys. Rev. Lett.* **89**, 056402 (2002).